

Ambivalent Intercalators for DNA: L-Shaped Platinum(II) Complexes

Matteo Cusumano,[†] Maria Letizia Di Pietro,[†] Antonino Giannetto,[†] Francesco Nicolò,[†] Bengt Nordén,[‡] and Per Lincoln^{*‡}*Dipartimento di Chimica Inorganica, Chimica Analitica e Chimica Fisica, University of Messina, 98166 Messina, Italy, and the Department of Physical Chemistry, Chalmers University of Technology, S-412 96 Gothenburg, Sweden*

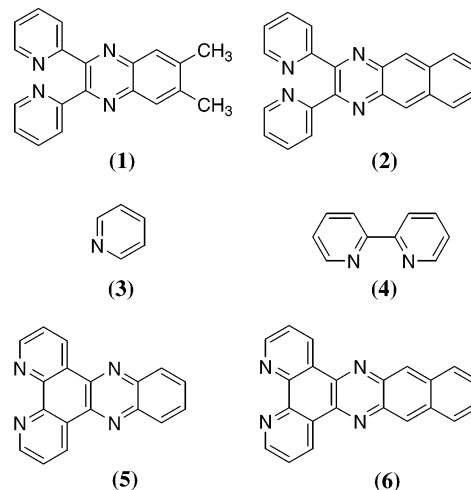
Received August 29, 2003

Novel platinum(II) square planar coordination complexes, in which two heteroaromatic ligands are held by the metal in an unusual L-shaped geometry orthogonal to each other, have been synthesized, and their interaction with DNA was investigated with absorption and linear dichroism spectroscopy. As a rule, the ligand that is coplanar with the coordination square of Pt is found to be oriented perpendicular relative to the DNA helix axis when bound, suggestive of its intercalation between the base pairs of DNA. However, when this coplanar ligand is replaced by two pyridines, the opposite ligand, orthogonal to the coordination square, is instead preferentially intercalated. This behavior shows that these new complexes do indeed show some properties of true ambintercalators, i.e., compounds that can bind by intercalation of either of two distinct aromatic moieties.

Introduction

The interaction of DNA with cationic platinum(II) square planar complexes containing aromatic ligands has been an active research area during the last twenty years.¹ For a number of reasons, these substances, which avidly bind to duplex DNA by intercalation,² lend themselves to the study of the basic features of this type of noncovalent interaction. Platinum(II) complexes are thermodynamically stable and kinetically inert,³ their coordination geometry is more suitable than any other for intercalative binding; furthermore, using mixed ligand complexes, one can easily tune both the electronic and steric properties by using appropriate ligands or substituents at the ligands. As a rule the clashes of bulky ligands with the double helix do not prevent intercalation of the planar moiety.

Chart 1. Formulas of the Ligands Used



In this paper we present the results of a study of the interactions with double helix DNA of a series of mixed square planar platinum(II) complexes of the type [Pt(N–N)(N'–N')]²⁺ where one of the ligands is 6,7-dimethyl-2,3-bis(2-pyridyl)quinoxaline (DMeDPQ) (1) or 2,3-bis(2-pyridyl)benzo[g]quinoxaline (BDPQ) (2), and the other is either two pyridines (py) (3), 2,2'-bipyridine (bpy) (4), dipyrido[3,2-*a*:2'3'-*c*]phenazine (dppz) (5) or benzodipyrido[*b*:3,2-*h*:2'3'-*j*]phenazine (bdppz) (6) (Chart 1).

These substances have in common an unusual structural feature: coordination of the bis-(2-pyridyl) ligands 1 or 2

* Author to whom correspondence should be addressed. E-mail: lincoln@phc.chalmers.se.

[†] University of Messina.

[‡] Chalmers University of Technology.

- (1) Sundquist, W. I.; Lippard, S. J. *Coord. Chem. Rev.* **1990**, *100*, 293.
 (2) (a) Lippard, S. J. *Acc. Chem. Res.* **1978**, *11*, 211. (b) Cusumano, M.; Di Pietro, M. L.; Giannetto, A. *Chem. Commun.* **1996**, 2527. (c) Cusumano, M.; Di Pietro, M. L.; Giannetto, A.; Nicolò, F.; Rotondo, E. *Inorg. Chem.* **1998**, *37*, 563. (d) Liu, H.-Q.; Peng, S.-M.; Che, C. M. *Chem. Commun.* **1995**, 509. (e) Che, C. M.; Yang, M.; Wong, K.-H.; Chan, H.-L.; Lam, W. *Chem. Eur. J.* **1999**, *5*, 11.
 (3) (a) Basolo, F.; Pearson, R. G. *Mechanisms of Inorganic Reactions*; John Wiley: New York, 1968. (b) Wilkins, R. G. *Kinetics and Mechanisms of Reactions of Transition Metal Complexes*; VCH: Weinheim, Germany, 1991.

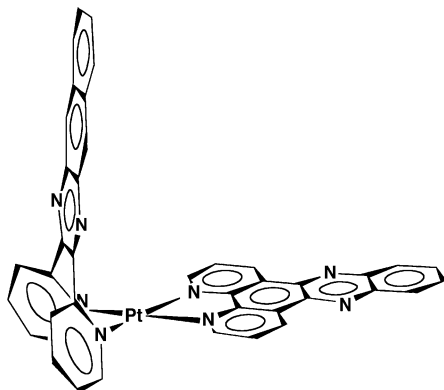


Figure 1. Schematic drawing of $[\text{Pt}(\text{BDPQ})(\text{dppz})]^{2+}$.

forces the quinoxaline moieties to be oriented almost perpendicularly to the square coordination plane of platinum (Figure 1).⁴

The potential interaction of these novel L-shaped complexes is, therefore, expected to be largely controlled by the steric interference of the ancillary ligands with the double helix. This should be especially true for intercalative interaction when part of the aromatic surface of the substance must be inserted within the core of the duplex between two adjacent base pairs. In this respect these complexes resemble octahedral complexes with rigid aromatic ligands where the steric clashes of the ancillary ligands with the sugar-phosphate backbone of the double helix control the interaction, leading, in the case of some chiral complexes, to enantioselective DNA binding properties.⁵

A further reason of interest in these complexes is that, when the second ligand is bpy, dppz, or bdppz, two potentially intercalating units are bound to the metal center. The aim of this work is to characterize the interacting moiety of these “ambintercalating” drugs and study the factors that favor its intercalation between the base pairs.

Experimental Section

Chemicals. Calf thymus DNA was purchased from Sigma Chemical Co. and purified as previously described,⁶ except in the case of the linear dichroism experiments for which it was directly dissolved in buffer and filtered through a 0.8- μm Millipore filter. Its concentration, expressed in bases, was determined spectrophotometrically using the molar absorptivity $6600 \text{ M}^{-1} \text{ cm}^{-1}$ (258 nm).⁷

NaCl and other chemicals were of reagent grade and were used without further purification.

$[\text{Pt}(\text{N}-\text{N})(\text{bpy})](\text{PF}_6)_2$ (N-N = DMeDPQ (Aldrich) or BDPQ⁸) were synthesized by suspending a slight excess of $[\text{Pt}(\text{bpy})\text{Cl}_2]$ ⁹ in

a $\text{CH}_3\text{OH}/\text{H}_2\text{O}$ 1:1 mixture in which the N-N ligand had been previously dissolved. The mixture was then heated to boiling and kept refluxing till almost complete dissolution of the suspension. The traces of solid material were eliminated by filtration and the final products were precipitated with an excess of NH_4PF_6 . Both complexes were recrystallized from CH_3OH .

$[\text{Pt}(\text{N}-\text{N})(\text{py})_2](\text{PF}_6)_2$ (N-N = DMeDPQ or BDPQ) were synthesized in a similar way by suspending $[\text{Pt}(\text{N}-\text{N})\text{Cl}_2]$ in H_2O and adding pyridine in large excess.

$[\text{Pt}(\text{N}-\text{N})(\text{N}'-\text{N}')](\text{PF}_6)_2$ (N-N = DMeDPQ or BDPQ; N'-N' = dppz¹⁰ or bdppz¹¹) were prepared starting from the corresponding dppz or bdppz platinum dichloride complex, obtained as follows. The phenazine ligand was reacted with an equivalent amount of $[\text{Pt}(\text{DMSO})_2\text{Cl}_2]$, both dissolved in warm DMSO. The phenazine dichloride complex, which precipitated, was isolated by filtration and washed several times with H_2O and CH_3OH to eliminate the DMSO. The dichloride was then added in slight excess to the N-N ligand solution in a $\text{CH}_3\text{OH}/\text{H}_2\text{O}$ 2:1 mixture. A few drops of DMSO were also added to facilitate the dissolution of the sparingly soluble phenazine dichloride complex, and the mixture was heated to boiling and refluxed for 3 days. After the mixture cooled, insoluble material was separated by centrifugation, and $[\text{Pt}(\text{N}-\text{N})(\text{N}'-\text{N}')](\text{PF}_6)_2$ was precipitated by adding an excess of NH_4PF_6 to the clear solution. Because the yield of the reaction was very low, it was necessary to repeat the treatment several times with the N-N ligand under the same conditions. $[\text{Pt}(\text{N}-\text{N})(\text{N}'-\text{N}')](\text{PF}_6)_2$ were crystallized from CH_3CN .

All the complexes were characterized by elemental analysis and ¹H and ¹³C NMR. $[\text{Pt}(\text{BDPQ})(\text{bpy})](\text{PF}_6)_2$ was also characterized in solid by single-crystal X-ray analysis.

Methods. All experiments were carried out at 25 °C and pH 7, in $1 \times 10^{-3} \text{ M}$ phosphate buffer and enough NaCl to give the desired ionic strength. Unless otherwise noted, the concentration of platinum complex was around $2.0 \times 10^{-5} \text{ M}$ in the spectroscopic studies. pH was measured with a Radiometer PHM 62. Absorption spectra were recorded using a Lambda 5 Perkin-Elmer or a Cary 4 Bio (Varian) spectrophotometer. ¹H and ¹³C spectra were recorded on a Bruker ARX-300 spectrometer.

Linear Dichroism. Linear dichroism (LD) spectra were recorded on a J-720 (Jasco) spectropolarimeter, equipped and used as described elsewhere.¹² The DNA was oriented by a flow gradient in a Couette cell with rotating outer cylinder.^{13a,b}

Analysis of LD and Absorption Spectra. Treating the isotropic absorption spectrum, at any wavelength λ , as a sum of contributions from purely polarized absorption bands $a(\lambda)_i$

$$A_{\text{iso}}(\lambda) = \sum a(\lambda)_i \quad (1)$$

the linear dichroism spectrum can be written as a *weighted* sum of the same purely polarized absorption bands

$$\text{LD}(\lambda) = S \sum w_i a(\lambda)_i \quad 0 < S < 1 \quad (2)$$

where S denotes an orientation factor, describing the degree of orientation of the system, and the weight w_i depends on the angle α_i between the orientation axis (here the DNA helix axis) and a transition moment of $a(\lambda)_i$

- (4) (a) Nicolò, F.; Cusumano, M.; Di Pietro, M. L.; Scopelliti, R.; Bruno, G. *Acta Crystallogr., Sect. C: Cryst. Struct. Commun.* **1998**, *54*, 485. (b) Escurer, A.; Comas, T.; Ribas, J.; Vicente, R.; Solans, X.; Zanchini, C.; Gatteschi, D. *Inorg. Chim. Acta* **1989**, *162*, 97. (5) (a) Nordén, B.; Tjerneld, F. *FEBS Lett.* **1976**, *67*, 368. (b) Barton, J. K.; Goldberg, J. M.; Kumar, C. V.; Turro, N. J. *J. Am. Chem. Soc.* **1986**, *108*, 2081. (c) Hiort, C.; Lincoln, P.; Nordén, B. *J. Am. Chem. Soc.* **1993**, *115*, 3448. (d) Önfelt, B.; Lincoln, P.; Nordén, B. *J. Am. Chem. Soc.* **2001**, *123*, 3630. (6) Cusumano, M.; Giannetto, A. *J. Inorg. Biochem.* **1997**, *65*, 137. (7) Felsenfeld, G.; Hirschman, S. Z. *J. Mol. Biol.* **1965**, *13*, 409. (8) Vogler, L. M.; Franco, C.; Jones, S. W.; Brewer, K. J. *Inorg. Chim. Acta* **1994**, *221*, 55. (9) Morgan, G. T.; Burstall, F. H. *J. Chem. Soc.* **1934**, 965.

- (10) Dickenson, J. E.; Summers, L. A. *Aust. J. Chem.* **1970**, *23*, 1023. (11) Lincoln, P.; Broo, A.; Nordén, B. *J. Am. Chem. Soc.* **1996**, *118*, 2644. (12) (a) Nordén, B.; Davidsson, A. *Tetrahedron Lett.* **1972**, *30*, 3093. (b) Nordén, B.; Tjerneld, F. *Chem. Phys. Lett.* **1977**, *50*, 508. (c) Nordén, B.; Seth, S. *Appl. Spectrosc.* **1985**, *39*, 647. (13) (a) Nordén, B.; Kubista, M.; Kurucsev, T. *Q. Rev. Biophys.* **1992**, *25*, 51. (b) Nordén, B.; Kurucsev, T. *J. Mol. Recognit.* **1994**, *7*, 141.

$$w_i = 3/2(3\cos^2\alpha_i - 1) \quad (3)$$

The reduced linear dichroism is the LD divided by the isotropic absorption

$$\text{LD}^r(\lambda) = \text{LD}(\lambda)/A_{\text{iso}}(\lambda) \quad (4)$$

and in regions of the spectrum where only a single polarization contributes, the LD^r becomes a wavelength-independent constant

$$\text{LD}^r = Sw_i \quad (5)$$

with the limits $-3S/2$ for a transition moment oriented perpendicular to the orientation axis and $+3S$ for a transition moment oriented parallel to it. Because of the large excess of DNA in the drug-DNA samples, the strong in-plane polarized $\pi \rightarrow \pi^*$ transitions of the nucleobases were totally dominating around 260 nm, and the orientation factor S could thus be determined under the assumption of an idealized B-form geometry of the DNA there $\alpha_{\pi \rightarrow \pi^*} = 90^\circ$.

When the dominating transitions only represent two angles α_i , as in most of the present cases, where the only strong absorption bands are due to $\pi \rightarrow \pi^*$ transitions polarized along the long axis of the ligands, the corresponding purely polarized absorption bands can be obtained from two linear combinations of isotropic absorption and linear dichroism spectra as follows:

$$a(\lambda)_1 = (w_2 A_{\text{iso}}(\lambda) - \text{LD}(\lambda)/S)(w_2 - w_1)^{-1} \quad (6)$$

$$a(\lambda)_2 = (w_1 A_{\text{iso}}(\lambda) - \text{LD}(\lambda)/S)(w_1 - w_2)^{-1}$$

Thus, by finding the two linear combinations in which the features of either of the two $a(\lambda)_i$ vanishes, the weights w_1 and w_2 and the two component spectra can be found (TEM method).¹⁴

Thermal Denaturation Experiments. The thermal denaturation temperature of complex-DNA mixtures (1:20) was determined in 1×10^{-3} M phosphate buffer (pH 7) containing 7.8×10^{-6} M complex and 2×10^{-3} M NaCl. Melting curves were recorded at 260 nm on a Lambda 3A Perkin-Elmer spectrophotometer interfaced with a Macintosh LC computer. The temperature was increased at a rate of 0.5 °C/min by using a PTP-1 Peltier Perkin-Elmer temperature programmer.

Viscometry. A Cannon-Ubbelohde semi-microdilution viscometer (series 75, Cannon Instruments Co.), thermostatically maintained at 25 °C in a water bath, was used for viscosity measurements. The viscometer contained 2 mL of sonicated DNA solution (approximately 600 base pairs) in 1×10^{-3} M phosphate buffer (pH 7) and 1×10^{-2} M NaCl. The complex solution ($(1-2) \times 10^{-4}$ M), containing also DNA (8×10^{-4} M) at the same concentration as that in the viscometer, was delivered in increments of 50–80 μL from a micropipet. Solutions were freed of particulate material by passing them through Acrodisc CR PTFE syringe filters before use. Flow times were measured by hand with a digital stopwatch. Reduced viscosities were calculated by established methods and plotted as $\ln\eta/\eta^\circ$ against $\ln(1 + 2r)$ (η is the intrinsic viscosity of the DNA solution in the presence of complex; η° the intrinsic viscosity of the DNA solution in the absence of complex; and r is $[\text{complex}]_{\text{bound}}/[\text{DNA}]_{\text{tot}}$). Under experimental conditions of low ionic strength and large $[\text{DNA}]/[\text{complex}]$ ratio the complex is totally bound and $[\text{complex}]_{\text{bound}}$ coincides with $[\text{complex}]_{\text{tot}}$.

X-ray Data Collection and Structure Determination. Crystal Data: $\text{C}_{32}\text{H}_{22}\text{F}_{12}\text{N}_6\text{P}_2\text{Pt}$, fw = 975.59, triclinic space group $P2_1/c$,

$a = 8.8598(7)$ Å, $b = 10.4745(7)$ Å, $c = 38.175(3)$ Å, $\beta = 95.102(6)^\circ$, $V = 3528.7(5)$ Å³, $Z = 4$, $F(000) = 1888$, $\rho = 1.836$ g/cm³, $\lambda = \text{Mo K}\alpha$ (0.71073 Å), $\mu = 41.64$ cm⁻¹.

Diffraction data of a yellow $0.38 \times 0.20 \times 0.15$ mm³ irregular crystal were collected at room temperature on a Siemens P4 automatic four-circle diffractometer¹⁵ using graphite-monochromated Mo K α radiation. Lattice parameters were obtained from least-squares refinement of the setting angles of 90 reflections with $5^\circ \leq 2\theta \leq 26^\circ$. A light crystal deterioration was revealed during the data collection by the 5% of intensity decreasing of the check reflections. The reflection intensities, collected up to $2\theta = 55^\circ$ by constant speed ω scan technique, were evaluated by a profile fitting among 2θ shell procedure¹⁶ and then corrected for Lorentz-polarization effects. An absorption correction was applied by fitting a pseudo-ellipsoid to the azimuthal scan data of 10 high- χ reflections¹⁷ ($T_{\text{max/min}} = 0.57/0.30$). Data-reduction has been performed by using the SHELXTL package.¹⁸

The systematic absences and statistics $|E^2 - 1| = 0.925$ (expected 0.968 for centrosymmetric packing) pointed to the centric space group $P2_1/c$. The crystal structure was solved by standard Patterson methods and subsequently completed by a combination of least-squares techniques and Fourier syntheses. H atoms were included in the refinement among the "riding model" method with the X-H bond geometry and the H isotropic displacement parameter depending on the parent atom X. The refinement, with all nonhydrogen atoms anisotropic and minimizing the function $\sum w(F_o^2 - F_c^2)^2$, was carried out by the full-matrix least-squares technique, based on all independent 8100 F^2 , with SHELXL97.¹⁹ The model converged to the final residual $R1(\text{obsd/all}) = 0.0526/0.0919$, $wR2(\text{obsd/all}) = 0.1289/0.1540$ (where $\text{obsd} = 5235$ reflections with $I = 2\sigma(I)$) and goodness-of-fit = 1.023. Both PF₆⁻ anions appeared to be affected by a significant rotational disorder as evidenced by the large fluorine thermal ellipsoids, but any attempt to split their orientations was unsuccessful. In the last difference Fourier map the significant density residuals were up to 1.1 e Å⁻³ at 1 Å from the Pt atom.

Final geometrical calculations and drawings were carried out with the PARST program²⁰ and the XP utility of the Siemens package, respectively. Selected geometry data of the molecule are listed in Table 1.

Results

Because of the coordination mode of DMeDPQ and BDPQ, all the complexes exhibit an angular L-shaped structure. The ligands DMeDPQ and BDPQ may bind metal ions^{4b,21} either through one pyrazine nitrogen and one pyridinenitrogen atom forming a five-membered ring, or through both pyridine nitrogen atoms disposed in a cis

(15) Siemens. XSCANS, PC-Dos version 2.2; Siemens Analytical X-ray Instruments Inc.: Madison, WI, 1996.

(16) Diamond, R. *Acta Crystallogr., Sect. A: Found Crystallogr.* **1969**, *25*, 43.

(17) Kopfmann, G.; Huber, R. *Acta Crystallogr., Sect. A: Found Crystallogr.* **1968**, *24*, 348.

(18) Sheldrick, G. M. SHELXTL, VMS version 5.05; Siemens Analytical X-ray Instruments Inc.: Madison, WI, 1991.

(19) Sheldrick, G. M. SHELXL97. Program for Crystal Structure Refinement.; University of Göttingen, Germany, 1997.

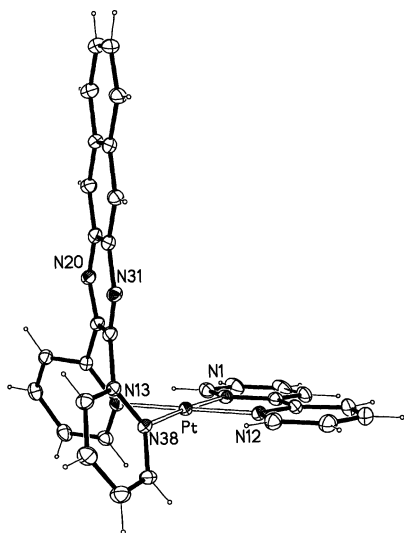
(20) Nardelli, M. *Comput. Chem.* **1983**, *7*, 95 (version locally modified).

(21) (a) Rillema, D. P.; Taghdiri, D. G.; Jones, D. S.; Keller, C. D.; Worl, L. A.; Meyer, T. J.; Levy, H. A. *Inorg. Chem.* **1987**, *26*, 578. (b) Goodwin, K. V.; Pennington, W. T.; Petersen, J. D. *Acta Crystallogr., Sect. C: Cryst. Struct. Commun.* **1990**, *46*, 898. (c) Escurer, A.; Vicente, R.; Comas, T.; Ribas, J.; Gomez, M.; Solans, X.; Gatteschi, D.; Zanchini, C. *Inorg. Chim. Acta* **1991**, *181*, 51.

(14) Michl, J.; Thulstrup, E. *Spectroscopy with Polarized Light*; VCH Publishers: New York, 1986; p 120.

Table 1. Selected Bond Lengths [Å] and Angles [°] for Compound [Pt(BDPQ)(bpy)](PF₆)₂

Pt–N(38)	2.011(7)	Pt–N(1)	2.014(7)
Pt–N(12)	2.026(7)	Pt–N(13)	2.030(7)
N(1)–C(6)	1.361(12)	C(7)–N(12)	1.355(11)
C(6)–C(7)	1.468(15)	N(13)–C(18)	1.352(10)
C(18)–C(19)	1.499(11)	C(19)–N(20)	1.311(10)
C(19)–C(32)	1.445(12)	N(20)–C(21)	1.382(11)
C(21)–C(30)	1.411(14)	C(30)–N(31)	1.369(10)
N(31)–C(32)	1.311(10)	C(32)–C(33)	1.475(11)
C(33)–N(38)	1.350(9)		
N(38)–Pt–N(12)	97.5(3)	N(1)–Pt–N(12)	80.9(3)
N(38)–Pt–N(13)	85.4(3)	N(1)–Pt–N(13)	96.2(3)
N(1)–C(6)–C(7)	114.4(8)	N(12)–C(7)–C(6)	115.8(8)
N(13)–C(18)–C(19)	120.3(7)	C(32)–C(19)–C(18)	125.3(7)
C(19)–N(20)–C(21)	117.2(8)	C(32)–N(31)–C(30)	118.4(8)
C(19)–C(32)–C(33)	125.3(7)	N(38)–C(33)–C(32)	120.7(7)
C(19)–C(32)–C(33)–N(38)	52(1)	N(13)–C(18)–C(19)–C(32)	–48(1)
N(1)–C(6)–C(7)–N(12)	3(1)		

**Figure 2.** View of the asymmetric unit of [Pt(BDPQ)(bpy)]²⁺ evidencing molecular shape. Thermal ellipsoids are drawn at 10% of probability while H size is arbitrary. Carbon numbering scheme and both PF₆[−] anions have been omitted for clarity.

conformation to form a seven-membered ring. The last binding mode is the one reported, so far, for mononuclear palladium(II)^{4a} and platinum(II)^{22,23} complexes. This type of coordination implies rotation of the pyridine groups toward the metal atom so that in the resulting complex the quinoxaline moiety lies almost perpendicularly to the square plane. Crystal structure determination for [Pt(BDPQ)(bpy)](PF₆)₂ shows that the two pyridine rings are rotated with respect to the tricycle system plane by 44.1(2) and 50.3(2)°, forming a dihedral angle of 101.4(2)°. Such a symmetric butterfly-like arrangement of the pyridine rings leads to four equivalent Pt–N bonds and to an almost regular square planar geometry of the metal (Figure 2).

The flat bipyridine chelating ligand lies on the Pt coordination plane and forms a dihedral angle of 90.05(7)° with the mean plane of the other ligand. The overall shape of the complex has a section similar to the character “L” where the longest side, represented by the benzoquinoline

fragment, has no significant steric hindrances by the rest of the molecule. In the solid state, the complex units are arranged in infinite columns by the alternate overlapping of parallel tricycle fragments of the cations. However, the adjacent plane separation of 3.94(4) Å is larger than the usual value denoting significant graphitic interaction (about 3.5 Å) (see Supporting Information).

Coordination of DMeDPQ and BDPQ in the other complexes reported has been established²³ by ¹H and ¹³C NMR.

All the complexes, which are very stable in a buffered aqueous solution (2.1 × 10^{−2} M NaCl in 1 × 10^{−3} M phosphate buffer), follow the Beer’s law throughout the concentration range used [(1–4) × 10^{−5} M]. Substantial absorption changes occur upon interaction immediately after mixing of the complexes with DNA. The inertness of the complexes studied, toward ligand substitution, rules out fast bond formation between platinum and DNA nucleophilic sites suggesting a noncovalent character of the DNA–complex interaction. This is further confirmed by the reversibility of the spectral variations, observed in most cases, on increasing ionic strength.

Spectrophotometric titration of [Pt(DMeDPQ)(bpy)]²⁺ and [Pt(BDPQ)(bpy)]²⁺ with DNA was associated with hypochromicity and shift to the red; well kept isosbestic points were observed till the end of the titration (not shown). Spectral variations, characterized by isosbestic points, were observable also for the complexes [Pt(BDPQ)(py)₂]²⁺ and [Pt(DMeDPQ)(py)₂]²⁺; however, in the latter case no appreciable shift to the red is associated with the hypochromism (not shown). For the complexes containing the extended phenanthrolines dppz and bdppz spectral changes were more complicated and depend on the [complex]/[DNA] ratio. Spectrophotometric titrations of these complexes with DNA lead to two distinct variations: at low [DNA] values the absorption maxima show large hypochromism without significant bathochromism, but as the titration proceeds there is a substantial shift to longer wavelengths (not shown). These effects close to saturation are likely due to interchromophore interactions between adjacently bound complexes on DNA, which are not unlikely given the size of these complexes, that can give rise to physical contacts even if complexes intercalate with nearest neighbor exclusion (see

(22) Granifo, J.; Vargas, M. E.; Rocha, H.; Garland, M. T.; Baggio, R. *Inorg. Chim. Acta* **2001**, *321*, 209–214.

(23) Cusumano, M.; Di Pietro, M. L.; Rotondo, E. manuscript in preparation.

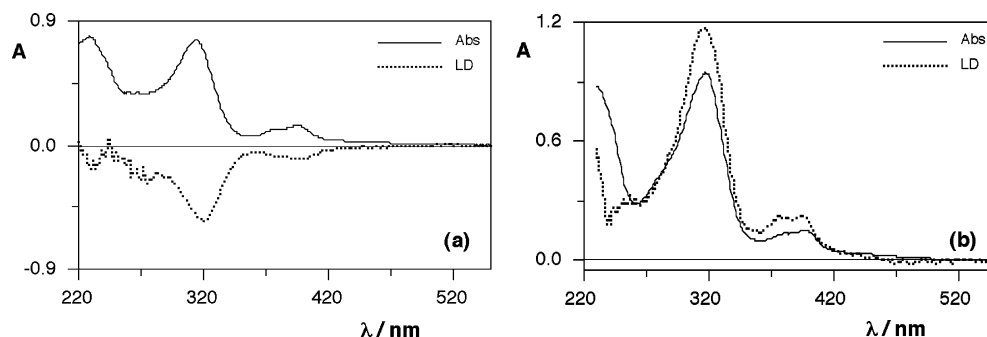


Figure 3. Isotropic absorption and flow linear dichroism spectra of (a) $[\text{Pt}(\text{BDPQ})(\text{py})_2]^{2+}$ at $[\text{DNA}]/[\text{complex}] = 40$ and (b) $[\text{Pt}(\text{BDPQ})(\text{bpy})]^{2+}$ at $[\text{DNA}]/[\text{complex}] = 11$ (phosphate buffer, 1×10^{-3} M; NaCl, 2.1×10^{-2} M). The DNA contributions to LD and Abs have been subtracted.

Table 2. Features of the Interactions of the Complexes with DNA

complex	ΔT_m °C ^a	slope of $\ln(\eta/\eta^0)$ against $\ln(1 + 2r)^b$	S/S_0^c	α_z^d	α_y
$[\text{Pt}(\text{DMeDPQ})(\text{bpy})]^{2+}$	7.0	1.23 (± 0.18)	0.80 ^e	26°	61° ^f
$[\text{Pt}(\text{DMeDPQ})(\text{dppz})]^{2+}$	8.4	2.01 (± 0.16)	1.14 ^e	0°	90°
$[\text{Pt}(\text{DMeDPQ})(\text{bdppz})]^{2+}$	6.4	1.28 (± 0.15)	1.18	0°	90°
$[\text{Pt}(\text{DMeDPQ})(\text{py})_2]^{2+}$	2.5	very small	0.87	<i>h</i>	
$[\text{Pt}(\text{BDPQ})(\text{bpy})]^{2+}$	8.9	1.03 (± 0.17)	0.75 ^e	34°	90° ^f
$[\text{Pt}(\text{BDPQ})(\text{dppz})]^{2+}$	6.9	1.36 (± 0.18)	1.12	0°	90°
$[\text{Pt}(\text{BDPQ})(\text{bdppz})]^{2+}$	6.0	very small	0.80	15°	90°
$[\text{Pt}(\text{BDPQ})(\text{py})_2]^{2+}$	5.8	1.01 (± 0.15)	0.94	<i>h</i>	

^a $\Delta T_m = T_m(\text{with ligand}) - T_m(\text{without ligand})$; uncertainty approximately ± 0.5 °C. ^b Value for the reference intercalator $[\text{Pt}(\text{bpy})(\text{py})_2]^{2+} = 1.43$ (± 0.18). ^c The relative orientation factor S/S_0 of the sample, compared to free DNA under the same conditions; uncertainty being approximately ± 0.05 . Values determined at $[\text{DNA}]/[\text{complex}] = 40$ unless otherwise noted. ^d Uncertainty in α -values being approximately $\pm 15^\circ$ for values close to 0° or 90° , and $\pm 5^\circ$ otherwise. ^e $[\text{DNA}]/[\text{complex}] = 11$. ^f The angle is for α_x . ^g $[\text{DNA}]/[\text{complex}] = 50$. ^h Incomplete binding precludes quantification of the angle, but negative sign of LD suggest intercalation of the quinoxaline ligand.

Figure 5). To avoid artifacts from interchromophore interaction, LD and corresponding isotropic absorption spectra were obtained with a large excess of DNA (at P/Pt of >40) for all complexes, except those containing bpy.

Changes in DNA melting temperature can give information on drug–DNA binding mode. As a rule DNA thermal stabilization is larger for intercalation than for external binding. However, in our case ΔT_m values (Table 2) are not particularly informative. The increase in DNA melting temperature for most of the complexes is intermediate between those reported²⁴ for intercalators and external binders bearing the same charge. The only exception is $[\text{Pt}(\text{DMeDPQ})(\text{py})_2]^{2+}$ for which thermal stabilization upon interaction is much lower than usually observed for intercalation, probably reflecting a rather low binding constant (see below).

Viscometric experiments also can give useful information on the binding mode of drugs to DNA; an increase in viscosity, normally observed upon intercalation, is due to unwinding of the double helix necessary to accommodate the intercalator. We have compared the increase in DNA viscosity for interaction of $[\text{Pt}(\text{bpy})(\text{py})_2]^{2+}$ and the complexes under study. The intercalating properties of $[\text{Pt}(\text{bpy})-$

$(\text{py})_2]^{2+}$ are well established.²⁵ Table 2 shows that, with the exception of $[\text{Pt}(\text{DMeDPQ})(\text{py})_2]^{2+}$ and $[\text{Pt}(\text{BDPQ})(\text{bdppz})]^{2+}$, the increase in DNA viscosity for the complexes investigated is comparable with that reported for the reference intercalator $[\text{Pt}(\text{bpy})(\text{py})_2]^{2+}$. The reason for the small effect on viscosity of $[\text{Pt}(\text{DMeDPQ})(\text{py})_2]^{2+}$ is likely due to low binding affinity (its LD signal is also quite small), whereas the small effect of $[\text{Pt}(\text{BDPQ})(\text{bdppz})]^{2+}$ is rather due to the lengthening of the DNA being counteracted by perturbation of the DNA structure by intercomplex interactions, as indicated by strong hypochromism close to saturation of DNA in the absorption titration (see above).

Because the L-shapes of the complexes can permit only one of the ligands to intercalate at a time, the question arises which of the two ligands is preferentially inserted into the DNA base stack, the ligand coplanar with the coordination square, or the bis(2-pyridyl)-substituted one?

Figure 3 shows the isotropic absorption and linear dichroism spectra of (a) $[\text{Pt}(\text{BDPQ})(\text{py})_2]^{2+}$ and (b) $[\text{Pt}(\text{BDPQ})(\text{bpy})]^{2+}$ bound to DNA.

All four spectra have very similar shapes, which indicates that the long axis polarized $\pi \rightarrow \pi^*$ transitions of the BDPQ ligand dominate. With two pyridines as additional ligands, the LD is clearly negative, although the LD^f is somewhat less negative at 320 and 400 nm than at the DNA band at 260 nm (data not shown). The LD^f value is probably affected by the presence of unbound complex, and we assign an intercalative binding mode to the BDPQ ligand. In vivid contrast, with 2,2'-bipyridine as additional ligand, the LD is strongly positive. We calculate an angle around 34° between the BDPQ ligand long axis and the DNA helix axis, which definitely excludes its intercalation (see Table 2). Because this axis is normal to the bipyridine plane, the data suggest that here instead the latter ligand can be intercalating, although with a pronounced tilt. The weights obtained from a resolution of the spectra into bipyridine and BDPQ absorption components (see Methods section) indicate that the tilt is largely a rotation about the 2-fold axis of the bipyridine ligand (data not shown).

Figure 4a shows the isotropic absorption and linear dichroism spectra of $[\text{Pt}(\text{DMeDPQ})(\text{bdppz})]^{2+}$, and the LD^f curve is shown in Figure 4b.

(24) (a) McCoubrey, A.; Latham, H. C.; Cook, P. R.; Rodger, A.; Lowe, G. *FEBS Lett.* **1996**, *380*, 73. (b) Cusumano, M.; Di Pietro, M. L.; Giannetto, A.; Messina, M. A.; Romano, F. *Chem. Commun.* **1999**, 1495.

(25) Cusumano, M.; Di Pietro, M. L.; Giannetto, A. *Chem. Commun.* **1996**, 2527.

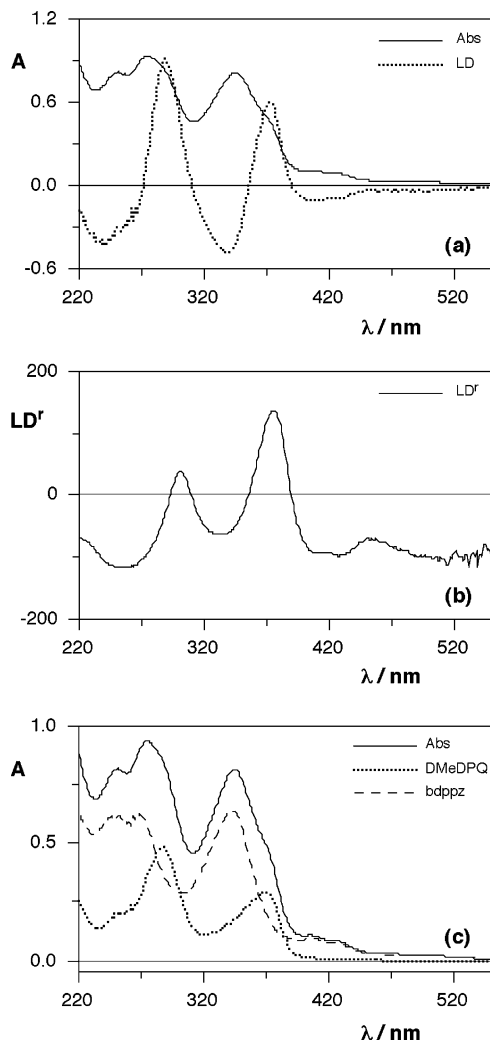


Figure 4. Isotropic absorption, linear dichroism, and LD^r for $[Pt-(DMeDPQ)(bdppz)]^{2+}$: (a) isotropic absorption and flow linear dichroism spectra (the DNA contributions have been subtracted); (b) reduced linear dichroism (LD^r , calculated from spectra without subtraction of the DNA contribution, arbitrary units); and (c) resolved polarized absorption components for $[Pt-(DMeDPQ)(bdppz)]^{2+}$ at $[DNA]/[complex] = 40$ (phosphate buffer, 1×10^{-3} M; NaCl, 2.1×10^{-2} M), obtained from the spectra in (a) according to eq 6.

The roller-coaster shape of the LD, contrasting the smooth profiles of the BDPQ-complexes with py or bpy in Figure 3, suggest very different orientations of the bdppz and DMeDPQ ligands, the former being perpendicularly oriented, i.e., intercalated, whereas the latter appears oriented parallel to the helix axis. Figure 4c shows the resolution into the individual absorption envelopes of orthogonal polarization from which the angle α in Table 2 was calculated for $[Pt-(DMeDPQ)(bdppz)]^{2+}$. Similarly, absorption and LD spectra for the other complexes were deconvoluted (see Supporting Information), under the constraint that ligand absorption components should be as invariant as possible between different complexes, giving the calculated angles in Table 2.

The LD results clearly show that in both the DMeDPQ and the BDPQ series, the bidentate ligand coplanar with the platinum coordination square is the one preferentially

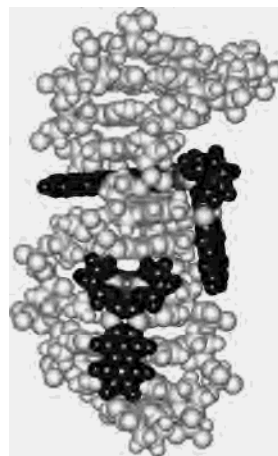


Figure 5. Molecular model for intercalation of two $[Pt(BDPQ)(bdppz)]^{2+}$ complexes into a DNA double-helix. The model was obtained with a limited energy-minimization using the Amber force field in the HyperChem software package. However, it should be noted that geometry of the complex was not minimized but modeled so as to correspond as closely as possible to the crystallographic structure of $[Pt(BDPQ)(bpy)](PF_6)_2$.

intercalated, no matter its size, although for the $[Pt-(DMeDPQ)(bpy)]^{2+}$ complex the data suggest a quite substantial unsymmetrical tilt of the whole bpy-plane. Only when two pyridine ligands are coordinated does the bis(pyridyl)-substituted ligand intercalate. A coarse molecular modeling of the intercalation of the $[Pt(BDPQ)(bdppz)]^{2+}$ complex suggests that, due to the sterical hindrance of the two noncoplanar pyridyl rings, the positively charged platinum center would have to be placed further away from the negatively charged phosphate groups in case of intercalation of the BDPQ end compared to if the bdppz end would intercalate (Figure 5).

The model further suggests that nonintercalated ligands from adjacently (nearest neighbor exclusion) intercalated complexes could physically interact. Such interactions may explain the findings, especially in the BDPQ series, of apparent intercomplex interactions at high binding ratios and the absence of clear isosbestic points.

The model also offers a rational explanation to the somewhat larger α_z angles for the bipyridine complexes: the longer ligands (dppz and bdppz) may allow the BDPQ or DMeDPQ part to avoid sterical clashes by placing them at, or slightly above, the mouth of the groove; whereas with bipyridine, this is not possible, and the BDPQ or DMeDPQ ligand must to some extent follow the contours of the groove with a tilt along the x axis as consequence.

Acknowledgment. This work was supported by MURST.

Supporting Information Available: Isotropic absorption and flow linear dichroism spectra; resolved polarized absorption components by the TEM method; a different view of the asymmetric unit and the crystal packing of $[Pt(BDPQ)(bpy)](PF_6)_2$ (pdf). This material is available free of charge via the Internet at <http://pubs.acs.org>.

IC035016F